

Is Orbital Angular Momentum (OAM) Based Radio Communication an Unexploited Area?

Ove Edfors, *Member, IEEE*, and Anders J. Johansson, *Member, IEEE*

Abstract—We compare the technique of using the *orbital angular momentum* (OAM) of radio waves for generating multiple channels in a radio communication scenario with traditional *multiple-in-multiple-out* (MIMO) communication methods. We demonstrate that, for certain array configurations in free space, traditional MIMO theory leads to eigen-modes identical to the OAM states. From this we conclude that communicating over the sub-channels given by OAM states is a subset of the solutions offered by MIMO, and therefore does not offer any additional gains in capacity.

Index Terms—Antenna arrays, antenna radiation patterns, channel capacity, free-space propagation, MIMO, orbital angular momentum, radio communication.

I. INTRODUCTION

IT WAS RECENTLY shown that the photon *orbital angular momentum* (OAM) can be used in the low frequency radio domain and is not restricted to the optical frequency range [1]. These findings and the claimed prospects for opening a new frontier in wireless communications, with “promise for the development of novel information-rich radar and wireless communication concepts and methodologies” [1], motivates the investigation in this paper.

Here we focus on the wireless communication aspects of [1] and the follow-up paper [2]. We start by identifying the conditions under which electromagnetic waves with specific OAM characteristics¹ are generated in [1], [2] and continue by comparing with properties of traditional communication using *multiple-in-multiple-out* (MIMO) antenna systems [5]–[7]. We pay special attention to the *singular value decomposition* (SVD) based derivation of channel capacity for MIMO systems [8], when applied to MIMO systems under free-space propagation conditions. Spatial multiplexing under free-space conditions may seem like a contradiction, but this very concept has been investigated in various forms for almost a decade [9]–[12]. When restricting ourselves to using circular antenna arrays, the SVD-based analysis in combination with properties of circulant

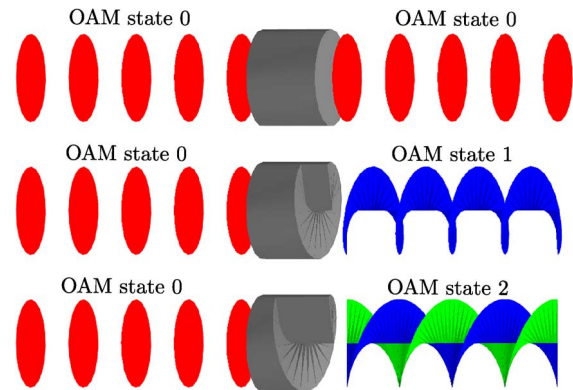


Fig. 1. Illustration of the creation of Laguerre-Gaussian laser beams from planar laser beams by using transparent spiral phase plates introducing a linear phase delay with azimuthal angle. OAM state k implies a $2\pi k$ phase delay over one revolution. Three different phase plates are illustrated in gray, for OAM state 0, 1 and 2. The colored surfaces are contour surfaces indicating where the phase of the laser beams is zero.

matrices [13], [14] can deliver the same beam-forming and the same OAM properties as in [1], [2]. The beam forming process for all eigenmodes/OAM states can be performed by a *discrete Fourier transform* (DFT) [15], which was also observed in [1]. The analysis also reveals that the eigenmodes of the resulting MIMO system are not necessarily unique, making OAM radio communication a sub-class of traditional MIMO communication with circular antenna arrays. Finally, we conclude the analysis by comparing the channel capacity of OAM-based communication, resulting from MIMO with circular antenna arrays, with known limits on the capacity of MIMO communication [7]. This shows that OAM based communication can achieve nearly optimal capacity gain, as predicted by MIMO theory, when the antenna arrays are closely spaced compared to the Rayleigh distance.

II. SHORT REVIEW OF RADIO OAM

Radio OAM can be seen as a development of techniques used in laser optics, where Laguerre–Gaussian (LG) mode laser beams are created using spiral phase plates [16]. The phase fronts of the created LG beams are helical in the sense that the phase front varies linearly with azimuthal angle, as illustrated in Fig. 1.

As a means of creating radio waves with OAM properties the authors of [1] and [2] use antenna arrays consisting of concentric *uniform circular arrays* (UCAs). The antenna elements in the UCAs are fed with the same input signal, but with a successive delay from element to element such that after a full turn the phase has been incremented by an integer multiple k of 2π . The basic principle of one of these UCAs is shown in Fig. 2.

Manuscript received February 24, 2011; revised May 26, 2011; accepted July 15, 2011. Date of publication October 24, 2011; date of current version February 03, 2012.

The authors are with the Department of Electrical and Information Technology, Lund University, 221 00 Lund, Sweden (e-mail: ove.edfors@eit.lth.se; ajn@es.lth.se).

Color versions of one or more of the figures in this paper are available online at <http://ieeexplore.ieee.org>.

Digital Object Identifier 10.1109/TAP.2011.2173142

¹These radio waves with specific OAM characteristics are often called “twisted radio beams” [3], [4] in popular science contexts.

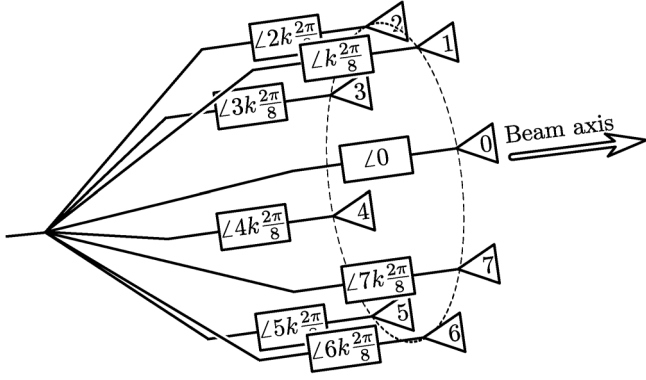


Fig. 2. Eight-element UCA with phase rotation $nk2\pi/8$ on element n to approximate OAM state k .

In [1] they calculate the far-field intensity patterns using NEC2 [17] and conclude that the results are very similar to those obtained in paraxial optics. It is also pointed out that the different OAM states in a beam can be decomposed by integrating the complex field vector weighted with $\exp(-jk\phi)$ along a circle around the beam axis. In practice there will be a finite number of antennas in an UCA measuring the field and the integration operation is approximated by a *discrete Fourier transform* (DFT) of the field in the antenna positions (or the antenna outputs). In [1] it is also concluded that with a limited number of antennas, N , there is an upper limit on the largest OAM number k that can be resolved, namely $|k| < N/2$.

Before we investigate these array design strategies for approximating beams with certain OAM states and apply standard MIMO theory to the resulting systems, let us briefly review the basics of narrow-band MIMO systems.

Narrow-band MIMO systems have been addressed in numerous publications during the last decade and a standard formulation of the input/output relationship in complex base-band notation is

$$\mathbf{y} = \mathbf{H}\mathbf{x} + \mathbf{n} \quad (1)$$

where $\mathbf{x} \in \mathbb{C}^{N_{\text{TX}}}$ is the vector of N_{TX} inputs, $\mathbf{y} \in \mathbb{C}^{N_{\text{RX}}}$ the vector of N_{RX} outputs, $\mathbf{H} \in \mathbb{C}^{N_{\text{RX}} \times N_{\text{TX}}}$ the MIMO channel matrix, and $\mathbf{n} \in \mathbb{C}^{N_{\text{RX}}}$ the vector of additive receiver noise. In many cases \mathbf{H} is assumed to be random, e.g., in wireless MIMO communication scenarios with relative movements in the propagation environment. Here we assume that \mathbf{H} is both known and has specific properties. The additive noise \mathbf{n} is assumed to be a vector of independent and identically distributed (i.i.d.) zero-mean, circularly symmetric, complex Gaussian noise components such that $\mathbf{n} \sim N(\mathbf{0}, \sigma_n^2 \mathbf{I}_{N_{\text{RX}}})$, where σ_n^2 is the noise variance on each receiver branch and $\mathbf{I}_{N_{\text{RX}}}$ is the $N_{\text{RX}} \times N_{\text{RX}}$ identity matrix.

The channel capacity of the MIMO system above has been known for a long time, for both known and unknown channel at the transmitter side. We will review a technique here to derive the capacity of the system, first introduced by Telatar [8], which is essential to the analysis in the rest of the paper. We use the singular value decomposition (SVD) of the channel matrix

$$\mathbf{H} = \mathbf{U}\mathbf{\Sigma}\mathbf{V}^H \quad (2)$$

where $\mathbf{U} \in \mathbb{C}^{N_{\text{RX}} \times N_{\text{RX}}}$ and $\mathbf{V} \in \mathbb{C}^{N_{\text{TX}} \times N_{\text{TX}}}$ are unitary matrices containing the left and right singular vectors of \mathbf{H} , respectively, while $\mathbf{\Sigma} \in \mathbb{C}^{N_{\text{RX}} \times N_{\text{TX}}}$ is a diagonal matrix with the positive singular values $\mu_1, \mu_2, \dots, \mu_r$, in decreasing order, on its diagonal, and $r \leq \min(N_{\text{TX}}, N_{\text{RX}})$ is the rank of \mathbf{H} . The left and right singular vectors in \mathbf{U} and \mathbf{V} are obtained from the eigen-decompositions of the Hermitian matrices $\mathbf{H}\mathbf{H}^H$ and $\mathbf{H}^H\mathbf{H}$, respectively, while the singular values along the diagonal in $\mathbf{\Sigma}$ are the square roots of the corresponding eigenvalues ($\mathbf{H}\mathbf{H}^H$ and $\mathbf{H}^H\mathbf{H}$ share the same set of positive eigenvalues).

From a capacity point of view, nothing is changed if we perform pre-processing to obtain our transmitted vector \mathbf{x} with the unitary matrix \mathbf{V} , and post-processing of our received vector \mathbf{y} with the unitary matrix \mathbf{U}^H . To describe the pre- and post-processing, we use the notation

$$\mathbf{x} = \mathbf{V}\tilde{\mathbf{x}} \quad (3)$$

$$\tilde{\mathbf{y}} = \mathbf{U}^H\mathbf{y}. \quad (4)$$

The pre- and post-processing operations above can also be seen as receiver- and transmitter-side beam-forming, where the left and right singular vectors of the channel matrix \mathbf{H} are used as steering vectors. Performing these operations on the original MIMO system (1) gives us an equivalent system

$$\tilde{\mathbf{y}} = \mathbf{U}^H\mathbf{y} = \mathbf{U}^H(\mathbf{H}\mathbf{V}\tilde{\mathbf{x}} + \mathbf{n}) \quad (5)$$

$$= \mathbf{U}^H\mathbf{H}\mathbf{V}\tilde{\mathbf{x}} + \mathbf{U}^H\mathbf{n} = \mathbf{\Sigma}\tilde{\mathbf{x}} + \tilde{\mathbf{n}} \quad (6)$$

where we, in the last step, use the SVD in (2) and denote the noise by $\tilde{\mathbf{n}} = \mathbf{U}^H\mathbf{n}$. Since \mathbf{U} is unitary, the new noise vector has the same distribution as \mathbf{n} itself, i.e., $\tilde{\mathbf{n}} \sim N(\mathbf{0}, \sigma_n^2 \mathbf{I}_{N_{\text{RX}}})$.

The corresponding capacity C_k for known channel at the transmitter becomes

$$C_k = \sum_{i=1}^r \log_2 \left(1 + \frac{P_i}{\sigma_n^2 / \mu_i^2} \right) \text{ bit/sec/Hz} \quad (7)$$

where all the available power P is distributed across the channels, according to the water-filling principle, such that

$$P = \sum_{i=1}^r P_i. \quad (8)$$

III. CAPACITY OF FREE SPACE MIMO SYSTEMS

To be able to compare free space MIMO systems against each other we need the channel matrix \mathbf{H} in (1) for a given configuration of the antenna arrays and a measure which quantifies the performance of a particular configuration. We will use the channel capacity of the MIMO system, relative to the capacity of a *single-in-single-out* (SISO) system, operating at the same antenna separation and using the same total transmit power. We call this the *capacity gain* of the MIMO system over a SISO system.

A. Channel Matrices in Free Space

Given the distance d between a pair of antenna elements in free space, we denote the (narrow band) transfer function from transmit antenna input to receive antenna output as

$$h(d) = \beta \frac{\lambda}{4\pi d} \exp \left(-j2\pi \frac{d}{\lambda} \right) \quad (9)$$

where the free space loss is given by $\lambda/(4\pi d)$, the additional phase rotation due to propagation distance is introduced by the complex exponential term, λ denotes the wavelength of the used carrier frequency, and β contains all relevant constants such as attenuation and phase rotation caused by antennas and their patterns on both sides.

For the above model to be relevant in our analysis of antenna arrays, we assume that all antenna elements (in each array) are equal and that the propagation distance d is large enough to provide:

- a valid far-field assumption between any pair of transmit/receive antenna elements, and
- relative array sizes (diameters) small enough to assume that the antenna diagrams are constant over the directions of departure/directions of arrival involved.

The first of these requirements essentially says that the free-space loss formula should be valid, while the second one implies that the antenna diagrams of the used antenna elements should be *smooth enough* in the direction of the opposing array to allow them to be approximated well by a constant (included in β above). These requirements are not strictly necessary for the analysis, but greatly simplifies the expressions.

Given that we have an $N_{RX} \times N_{TX}$ MIMO system, where $d_{n_{RX}, n_{TX}}$ is the distance between receive antenna element n_{RX} and transmit antenna element n_{TX} , the channel matrix becomes

$$\mathbf{H} = \begin{bmatrix} h_{1,1} & h_{1,2} & \cdots & h_{1,N_{TX}} \\ h_{2,1} & h_{2,2} & \cdots & h_{2,N_{TX}} \\ \vdots & \vdots & \ddots & \vdots \\ h_{N_{RX},1} & h_{N_{RX},2} & \cdots & h_{N_{RX},N_{TX}} \end{bmatrix} \quad (10)$$

where

$$h_{n_{RX}, n_{TX}} = h(d_{n_{RX}, n_{TX}}) \quad (11)$$

is given by (9).

B. Capacity Gain

In the rest of the paper we will use a relative capacity measure to evaluate the gain of applying MIMO instead of SISO communication. We assume that we have equal transmitters and receivers for both systems, with the same antennas and equal receiver noise figures. The SISO system uses a single transmitter-receiver pair, while the MIMO system uses multiple units on each side.

As a basis for the capacity gain, we assume that our SISO system needs a certain transmit power P_{SISO} to achieve a certain SNR on the receiver side. The required transmit power can be calculated using a simple link budget. By using the propagation loss as given by (9), the required transmit power becomes

$$P_{SISO} = \text{SNR} \left(\frac{4\pi D}{\beta\lambda} \right)^2 \sigma_n^2 \quad (12)$$

where σ_n^2 is the receiver noise variance and D is the distance between the transmitting and receiving antenna. This choice of transmit power gives a reference SISO channel capacity of

$$C_{SISO}(P_{SISO}) = \log_2(1 + \text{SNR}) \text{ bit/sec/Hz.} \quad (13)$$

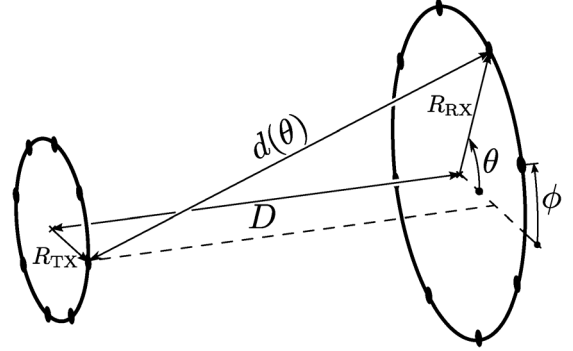


Fig. 3. Distance $d(\theta)$ between two antenna elements on concentric circles with radii R_{TX} and R_{RX} , respectively, placed on a common beam axis at a distance D from each other. The angle between first elements in the two arrays is denoted ϕ .

We now evaluate the capacity of the studied MIMO system for the same transmit power, $P_{MIMO} = P_{SISO}$, and compare their channel capacities. We define the *MIMO capacity gain* as

$$G_{MIMO} = \frac{C_{MIMO}(P_{SISO})}{C_{SISO}(P_{SISO})} = \frac{C_{MIMO}(P_{SISO})}{\log_2(1 + \text{SNR})} \quad (14)$$

where $C_{MIMO}(P_{SISO})$ is the channel capacity for the studied MIMO system for known channel at the transmitter, i.e., where $C_{MIMO}(P_{SISO})$ is given by C_k in (7).

Following the analysis in [7], the capacity gain of any MIMO system is limited by the number of antennas at each side as $G_{MIMO} \leq \min(N_{TX}, N_{RX})$.

Having established our metric for comparing the merits of different MIMO systems, we move on to the specific antenna array geometries addressed in this paper.

IV. CIRCULAR ARRAYS ON THE SAME BEAM AXIS IN FREE SPACE

The basic system configuration described in [1] concerns antenna arrays with one or more concentric UCAs used to create electric fields with different OAM states. Here we focus on the simplest MIMO system using such antenna structures; two UCAs facing each other on the same beam axis at a distance D . One is the transmitting array and one is the receiving array, as illustrated in Fig. 3, where the dots indicate antenna element positions. The distance between arbitrary points on the two concentric circles, with radii R_{TX} and R_{RX} , on which the antenna elements are placed, with an angle θ between the points is

$$d(\theta) = \sqrt{D^2 + R_{TX}^2 + R_{RX}^2 - 2R_{TX}R_{RX}\cos^2\theta}. \quad (15)$$

Assuming N_{TX} evenly distributed antennas on the first circle and N_{RX} evenly distributed antennas on the second circle, neighboring antenna elements on the two circles are

$$\Delta\theta_{TX} = \frac{2\pi}{N_{TX}} \quad \text{and} \quad \Delta\theta_{RX} = \frac{2\pi}{N_{RX}} \quad (16)$$

radians apart, respectively.

Without loss of generality, we can assume that the first antenna element on the first circle is placed at zero radians, while the first antenna element on the second circle is placed at an angle ϕ . By changing the value on ϕ we can obtain all possible

relative rotations between the two antenna arrays. Using the angles between two elements on each array as described in (16), while introducing a relative array rotation ϕ , the angle between transmit element n_{TX} and receive element n_{RX} becomes

$$\theta_{n_{\text{RX}}, n_{\text{TX}}} = 2\pi \left(\frac{n_{\text{RX}}}{N_{\text{RX}}} - \frac{n_{\text{TX}}}{N_{\text{TX}}} \right) + \phi \quad (17)$$

where $1 \leq n_{\text{TX}} \leq N_{\text{TX}}$ and $1 \leq n_{\text{RX}} \leq N_{\text{RX}}$.

If the distance D and the array radii R_{TX} and R_{RX} are given, the distance between elements in the two arrays can be expressed as, substituting (17) in (15),

$$d_{n_{\text{RX}}, n_{\text{TX}}} = d(\theta_{n_{\text{RX}}, n_{\text{TX}}}). \quad (18)$$

An important observation at this stage is that for the same number of antennas $N_{\text{TX}} = N_{\text{RX}} = N$ on both sides, the element-to-element distances $d_{n_{\text{RX}}, n_{\text{TX}}}$ only depend on the difference $(n_{\text{RX}} - n_{\text{TX}}) \bmod N$. This relation holds for all array separations D , array radii R_{TX} and R_{RX} , and angles ϕ between first elements.

Assuming that the antenna elements of both arrays are co-polarized,² we use the distances between transmit and receive antenna elements (18) and the free space transfer function (9), to express the elements of the MIMO channel matrix (10) as

$$h_{n_{\text{RX}}, n_{\text{TX}}} = h(d(\theta_{n_{\text{RX}}, n_{\text{TX}}})) . \quad (19)$$

For the same number of antennas $N_{\text{TX}} = N_{\text{RX}} = N$ on both sides the matrix \mathbf{H} becomes *circulant* [13], since its elements inherit the property that $d(\theta_{n_{\text{RX}}, n_{\text{TX}}})$ only depends on the difference $(n_{\text{RX}} - n_{\text{TX}}) \bmod N$, through (19). This implies that the channel matrix is diagonalized by the $N \times N$ unitary DFT matrix

$$\mathbf{T}_N = [t_{p,q}] \quad (20)$$

with entries

$$t_{p,q} = \frac{1}{\sqrt{N}} \exp \left(-j2\pi \frac{(p-1)(q-1)}{N} \right) . \quad (21)$$

With this notation we can write the eigen-decomposition as

$$\mathbf{H} = \mathbf{T}_N \mathbf{\Delta} \mathbf{T}_N^H \quad (22)$$

where $\mathbf{\Delta}$ contains the eigenvalues of the channel matrix. To change this into an SVD, where the singular values are real, non-negative, and sorted in decreasing order, we first modify the eigen-decomposition by rearranging the order of the eigen-vectors so that the eigenvalues are sorted according to decreasing magnitude. Denote this sorted eigen-decomposition

$$\mathbf{H} = \tilde{\mathbf{T}}_N \tilde{\mathbf{\Delta}} \tilde{\mathbf{T}}_N^H . \quad (23)$$

With this notation, the matrices in the SVD of the channel matrix (2) can be expressed:

$$\mathbf{U} = \tilde{\mathbf{T}}_N \mathbf{S} \quad (24)$$

$$\mathbf{\Sigma} = \text{abs}(\tilde{\mathbf{\Delta}}) \quad (25)$$

$$\mathbf{V} = \tilde{\mathbf{T}}_N \quad (26)$$

²Here we focus on a single polarization while, in principle, two independent MIMO systems can be achieved if we exploit both polarization states.

where \mathbf{S} is a diagonal matrix, with unit magnitude complex numbers as diagonal elements, used to rotate the complex eigenvalues into singular values on the positive real axis. If $\tilde{\delta}_k$ is the k th eigenvalue (diagonal element) in $\tilde{\mathbf{\Delta}}$, the k th diagonal element of \mathbf{S} is $s_k = \exp(j\angle \tilde{\delta}_k)$. By observing that both transmit- and receive-side beam-formers, (3) and (4), are given by the rearranged DFT in (23), we have verified that the linear phase rotations across UCAs proposed in [1] and [2] to approximate OAM states in radio beams coincide with the eigen-modes derived with standard MIMO theory for our free-space scenario.³

The circulant property also helps us in the calculation of singular values of the channel matrix, which are the magnitude of the DFT of the first column of \mathbf{H} , sorted in decreasing order.

V. WAVE FRONT PROPERTIES AND CHANNEL CAPACITY

After verifying that the free-space MIMO model gives the same beam-forming vectors as the ones proposed in [1], we also want to verify the phase properties of the wave front as predicted by this model. Using the steering vectors in (3), with $\mathbf{V} = \mathbf{T}_N$, we can calculate the received signal in a point in space as

$$e = \mathbf{G} \mathbf{T}_N \mathbf{e}_k \quad (27)$$

where \mathbf{G} is the channel matrix from the transmitter array elements to a single receiving antenna element in the investigated point in space, using (9), and \mathbf{e}_k is a vector with a single *one* in the position corresponding to the k th OAM state. In Fig. 4 we show the resulting phase plots for an 8-element transmit array. The phase plots are calculated for three different distances, 1/4, 4 and 400 times the Rayleigh distance for the entire antenna arrays⁴

$$d_R = \frac{L^2}{2\lambda} \quad (28)$$

where the aperture L is set to the transmit UCA diameter $2R_{\text{TX}}$. The plot shows that we do not have very clean helical phases below the Rayleigh distance, but the gains of several of the OAM states makes them useful for communication. When the distance increases above the Rayleigh distance, we observe much cleaner helical phases, but the normalized gains of all non-zero OAM states fall rapidly, since the rank of the channel matrix approaches one. This makes all but the zeroth OAM state essentially useless at these distances for communication at realistic SNRs. Several of the OAM states at $D = 400d_R$ are so weak that we can clearly observe numerical problems in the plots.

We have verified that our simple MIMO model generates the helical wave fronts expected in OAM, but at the same time, the pure OAM states are not necessarily unique in the sense that they provide the only set of eigenmodes for the channel. In the

³It can also be shown that if the number of antenna elements on one side is an integer multiple of the number of antennas on the other side, the resulting channel matrix becomes *rectangular circulant* [14] and the matrix containing the singular vectors corresponding to the side with fewer elements is a DFT matrix. The singular vectors on the other side, however, do not form a DFT matrix but can be described in closed form with harmonic functions.

⁴While the antenna arrays may be closer than the (array) Rayleigh distance, any pair of transmit/receive antenna elements of the arrays are considered to be at far field distances from each other.

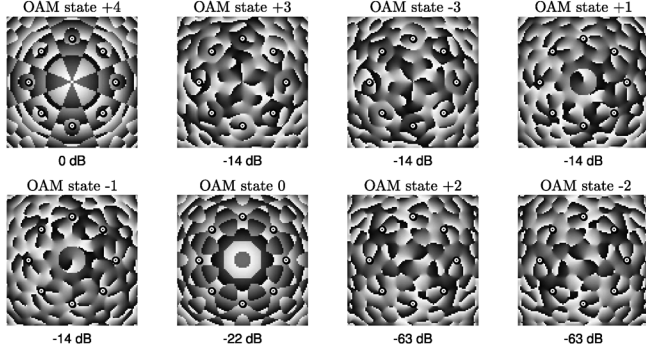
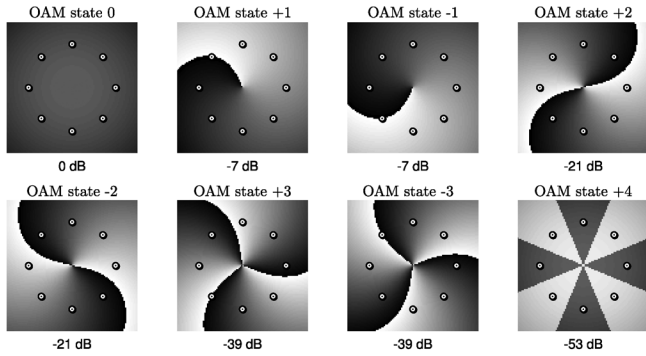
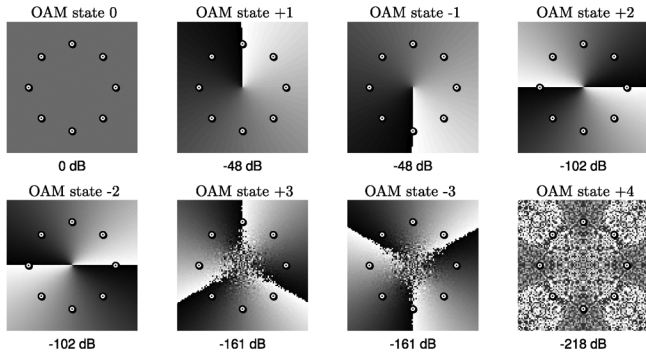
Phase diagrams at $D = d_R/4$ Phase diagrams at $D = 4d_R$ Phase diagrams at $D = 400d_R$ 

Fig. 4. Phase plots at three different distances from an 8-element UCA with radius of $R_{TX} = 100\lambda$. The DFT is used as transmit beam-former and phase plots are shown for distances of $1/4$, 4 and 400 times the Rayleigh distance $d_R = 20.000\lambda$. Phase is coded as shades of gray, from black to white representing the range $[-\pi, \pi]$, and the phase plots are sorted in order of gain (singular value). Normalized gains are shown below each phase plot and the plot area is $300\lambda \times 300\lambda$.

example provided in Fig. 4, there are singular values with multiplicity two, which leads to non-unique singular vectors. The non-uniqueness is illustrated by the phase plots in Fig. 5 for the same setup as in Fig. 4, but a numerical SVD is performed to obtain the eigenmodes rather than using the closed form expressions. Two of the eigenmodes (singular values of multiplicity one) coincide with OAM states 0 and $+4$ for $D = 400d_R$ in Fig. 4, while the other six display quite different characteristics (singular values with multiplicity 2). The set of singular values are the same for both cases, making them equivalent from a communication point of view.

When calculating the phase diagrams above, we notice that higher order OAM states become very weak beyond the

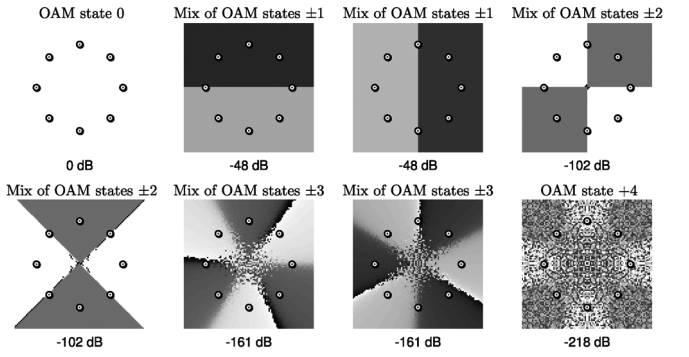
Phase diagrams at $D = 400d_R$ 

Fig. 5. Phase plots from an 8-element UCA with radius of $R_{TX} = 100\lambda$. A numerical SVD is performed of the channel, the right singular vectors are used as beam-formers and phase plots are shown for the distance 400 times the Rayleigh distance $d_R = 20.000\lambda$. Phase is coded as shades of gray, from black to white representing the range $[-\pi, \pi]$, and the phase plots are sorted in order of gain (singular value). Normalized gains are shown below each phase plot and the plot area is $300\lambda \times 300\lambda$.

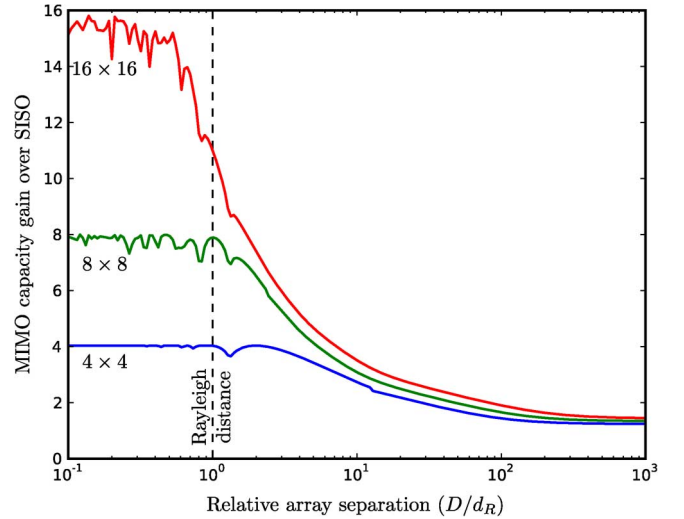


Fig. 6. Capacity gain over single antenna (SISO) system at UCA sizes 4×4 , 8×8 , and 16×16 , at an SNR of 30 dB. Curves are calculated for array radii 100λ and array separation distances from 10 times below to 1000 times above the Rayleigh distance (20.000λ).

Rayleigh distance. To investigate this further, we calculate the channel capacity gain, as defined in (14), for three different configurations with 4×4 , 8×8 , and 16×16 antenna elements, at a per-receiver branch SNR of 30 dB. The channel capacity for the MIMO configurations is maximized over all relative rotations ϕ of the two arrays. The results are shown in Fig. 6. We can see that in all three cases the capacity gain achieved by using OAM-based MIMO communication almost reach the theoretical maximum [7] of 4, 8, and 16 times that of a SISO system below the Rayleigh distance, while performance degrades considerably at larger distances. At 1000 times the Rayleigh distance only one eigen-mode (OAM state 0) is useful for communication and the only gain available is the the array gain. This behavior can also be understood from the radiation patterns displayed in [1] and [2], where all but OAM state 0 have a null in the forward direction.

VI. DISCUSSION AND CONCLUSION

In the investigation above, we have shown that OAM-based radio communication, as proposed in [1], can be obtained from standard MIMO theory, under certain conditions. Inspired by the discussion in [1], we made a system design with UCAs facing each other on the same beam axis in free space, which leads to circulant channel matrices, for all numbers of antenna elements (same number on both sides), all antenna radii (can be different at both ends), and all relative rotations of the arrays. Such matrices are diagonalized by the DFT, which means that the OAM states presented in [1] are one, not necessarily unique, set of eigen-modes of these channels.

In our evaluation of the expected performance of such systems we showed that well above the Rayleigh distance there is a single dominant eigen-mode/OAM state. This leads to only a small capacity gain over a SISO system, essentially due to the array gain. No multiplexing gain is achieved since only one of the modes will carry information at realistic SNRs. Well below the Rayleigh distance, the investigated systems almost achieve the maximum capacity gains predicted by MIMO theory when using the OAM based eigenmodes of the channels. This means that the system based on UCAs is a relatively good choice in free space, since there is very little extra gain to achieve with other array geometries. The helical phase of the OAM states remain coherent over vast distances, but the amount of energy that can be received beyond the Rayleigh distance with a limited-size array decays rapidly, as compared to free space attenuation, for all but OAM state 0. Since the Rayleigh distance increases with array radius and frequency, the distances at which we have a multiplexing gain can be increased with larger array radii or a move to higher frequencies. One application example would be to use the sub-millimeter range of wavelengths, where planar UCAs of reasonable size can be integrated into, e.g., wallpaper and used to provide short-range high data-rate links based on spatial multiplexing under free-space conditions in indoor environments.

Since transmitter and receiver beam-forming can be done with the DFT, OAM based communication between UCAs in free space has a potential to deliver high performance at short distances with a low computational complexity, when fast transforms are used. It is, however, only under very specific conditions that OAM based communication provides an optimal solution. The traditional and more general MIMO communication concept can handle all array geometries and propagation environments, including those where OAM based communication is optimal.

Our main conclusion is that exploiting OAM states does not bring anything conceptually new to the area of radio communications. It is well covered by traditional MIMO communication, using channel eigen-modes for transmission, in the sense that OAM states of radio waves will be automatically exploited whenever the array configurations and propagation environments call for it.

REFERENCES

- [1] B. Thidé, H. Then, J. Sjöholm, K. Palmer, J. Bergman, T. D. Carozzi, Y. N. Istomin, N. H. Ibragimov, and R. Khamitova, "Utilization of photon orbital angular momentum in the low-frequency radio domain," *Phys. Rev. Lett.*, vol. 99, no. 8, pp. 087701-1–087701-4, Aug. 2007.
- [2] S. M. Mohammadi, L. K. S. Daldorff, J. E. S. Bergman, R. L. Karlsson, B. Thidé, K. Forozesh, T. D. Carozzi, and B. Isham, "Orbital angular momentum in radio—A system study," *IEEE Trans. Antennas Propag.*, vol. 58, no. 2, pp. 565–572, Feb. 2010.
- [3] C. Barras, "Twisted radio beams could untangle the airwaves," *New Scientist* Mar. 2009 [Online]. Available: <http://www.newscientist.com/article/dn16591-twisted-radio-beams-could-untangle-the-airwaves.html>
- [4] E. Carlidge, "Adding a twist to radio technology," *Nature News* Feb. 2011 [Online]. Available: <http://www.nature.com/news/2011/110222/full/news.2011.114.html>
- [5] J. H. Winters, "On the capacity of radio communication systems with diversity in a rayleigh fading environment," *IEEE J. Sel. Areas Commun.*, vol. SAC-5, no. 5, pp. 871–878, Jun. 1987.
- [6] G. J. Foschini, "Layered space-time architecture for wireless communication in a fading environment when using multi-element antennas," *Bell Labs Tech. J.*, pp. 41–59, Autumn, 1996.
- [7] G. J. Foschini and M. J. Gans, "On limits of wireless communications in a fading environment when using multiple antennas," *Wireless Personal Commun.*, no. 6, pp. 311–335, 1998.
- [8] I. E. Telatar, "Capacity of multi-antenna Gaussian channels," *Eur. Trans. Telecommun.*, vol. 10, pp. 585–595, Sep. 1999.
- [9] J.-S. Jiang and M. A. Ingram, "Distributed source model for short-range MIMO," in *Proc. IEEE Veh. Tech. Conf.*, Orlando, FL, Oct. 2003, vol. 1, pp. 357–362.
- [10] F. Böhagen, P. Orten, and G. E. Öien, "Construction and capacity analysis of high-rank line-of-sight MIMO channels," in *Proc. IEEE Wireless Communications and Networking Conf. (WCNC)*, New Orleans, LA, Mar. 2005, vol. 1, pp. 432–437.
- [11] I. Sarris and A. R. Nix, "Design and performance assessment of maximum capacity MIMO architectures in line-of-sight," *IEEE Proc.-Commun.*, vol. 153, no. 4, pp. 482–488, Aug. 2006.
- [12] F. Böhagen, P. Orten, and G. E. Öien, "On spherical vs. plane wave modeling of line-of-sight MIMO channels," *IEEE Trans. Commun.*, vol. 57, no. 3, pp. 841–849, Mar. 2009.
- [13] P. J. Davies, *Circulant Matrices*, ser. Wiley-Interscience. New York: Wiley, 1979.
- [14] J. Fan, G. E. Stewart, and G. A. Dumont, "Two-dimensional frequency analysis for unconstrained model predictive control of cross-directional processes," *Automatica*, vol. 40, pp. 1891–1903, 2004.
- [15] A. V. Oppenheim and R. W. Schaffer, *Discrete-Time Signal Processing*, 2nd ed. Englewood Cliffs, NJ: Prentice Hall, 1999.
- [16] M. W. Beijersbergen, R. P. C. Coerwinkel, M. Kristensen, and J. P. Woerdman, "Helical-wavefront laser beams produced with a spiral phase plate," *Opt. Commun.*, vol. 112, pp. 321–327, Dec. 1994.
- [17] Numerical Electromagnetics Code. [Online]. Available: <http://www.nec2.org/>



Ove Edfors (M'00) received the M.Sc. degree in computer science and electrical engineering in 1990 and the Ph.D. degree in signal processing in 1996, both from Luleå University of Technology, Sweden.

In the spring of 1997, he worked as a researcher at the Division of Signal Processing at the same university, and in July 1997, he joined the staff at the Department of Electrical and Information Technology, Lund University, Sweden, where he has been a Professor of radio systems since 2002. His research interests include radio systems, statistical signal processing and low-complexity algorithms with applications in telecommunication.



Anders J. Johansson (M'03) received the Masters, Lic.Eng., and Ph.D. degrees in electrical engineering from Lund University, Lund, Sweden, in 1993, 2000, and 2004, respectively.

From 1994 to 1997, he was with Ericsson Mobile Communications AB developing transceivers and antennas for mobile phones. Since 2005, he has been an Associate Professor in the Department of Electrical and Information Technology, Lund University, Sweden. His research interests include antennas and wave propagation for medical implants as well as antenna systems and propagation modeling for MIMO systems.

He is involved as one of the researchers in the NeuroNano Research Center at Lund University, which is an interdisciplinary research initiative, and where he is responsible for the development of the telemetry part of the project.